AD-A041 305 CIVIL ENGINEERING LAB (NAVY) PORT HUENEME CALIF F/G 9/3
VALIDATION OF SIMULATION TECHNIQUES FOR ELECTROMECHANICAL COUPL--ETC(U)
MAY 77 K T HUANG, D M SHIROMA

UNCLASSIFIED CEL-TN-1484 NL

1 OF 1

AD
A041305

END

DATE
FILMED
7-77

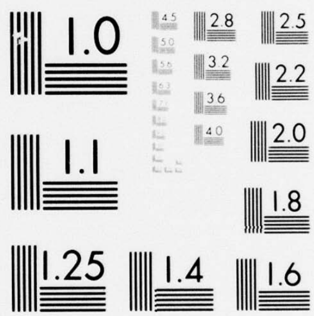

MICROCOPY RESOLUTION TEST CHART
NATIONAL BUREAU OF STANDARDS-1963-A

ADA041305

Technical Note

TN no. N-1484

title: VALIDATION OF SIMULATION TECHNIQUES FOR ELECTROMECHANICAL COUPLINGS IN ELECTRICAL MOTORS

author: K. T. Huang, Ph.D.
D. M. Shiroma

date: May 1977

sponsor: DIRECTOR OF NAVY LABORATORIES

program nos: Z-R000-01-142

CIVIL ENGINEERING LABORATORY
NAVAL CONSTRUCTION BATTALION CENTER
Port Hueneme, California 93043

Approved for public release; distribution unlimited.

Unclassified

SECURITY CLASSIFICATION OF THIS PAGE (When Data Entered)

REPORT DOCUMENTATION PAGE

READ INSTRUCTIONS BEFORE COMPLETING FORM

1. REPORT NUMBER TN-1484	2. GOVT ACCESSION NO. DN587002	3. RECIPIENT'S CATALOG NUMBER 9
4. TITLE (and Subtitle) VALIDATION OF SIMULATION TECHNIQUES FOR ELECTROMECHANICAL COUPLINGS IN ELECTRICAL MOTORS		5. TYPE OF REPORT & PERIOD COVERED Final; ~~FY-75 – FY-7T~~ 6. PERFORMING ORG. REPORT NUMBER
7. AUTHOR(s) K. T. Huang, Ph.D. and D. M. Shiroma		8. CONTRACT OR GRANT NUMBER(s) ZR00001
9. PERFORMING ORGANIZATION NAME AND ADDRESS CIVIL ENGINEERING LABORATORY Naval Construction Battalion Center Port Hueneme, California 93043		10. PROGRAM ELEMENT, PROJECT, TASK AREA & WORK UNIT NUMBERS 61152N; Z-R000-01-142
11. CONTROLLING OFFICE NAME AND ADDRESS Director of Navy Laboratories, Room 1062, Crystal Plaza Bldg. #5, Department of the Navy, Washington, D.C., 20360		12. REPORT DATE May 1977 13. NUMBER OF PAGES 23
14. MONITORING AGENCY NAME & ADDRESS (if different from Controlling Office)		15. SECURITY CLASS. (of this report) Unclassified 15a. DECLASSIFICATION DOWNGRADING SCHEDULE

16. DISTRIBUTION STATEMENT (of this Report)

Approved for public release; distribution unlimited.

17. DISTRIBUTION STATEMENT (of the abstract entered in Block 20, if different from Report)

18. SUPPLEMENTARY NOTES

391 111

19. KEY WORDS (Continue on reverse side if necessary and identify by block number)

High frequency injection, electromagnetic coupling, analog computer, electromechanical coupling, electrical power distribution.

20. ABSTRACT (Continue on reverse side if necessary and identify by block number)

High frequency injection and electromagnetic coupling techniques are used to measure the parameters of a single-phase induction motor to determine its equivalent circuit. This equivalent circuit is then programmed on the analog computer for verification. From the equivalent circuit, the electromechanical coupling which correlates the electrical and mechanical parameters can be determined. The analog simulation of the single-phase induction motor can then be used for experimentation, analysis, and design.

Unclassified

SECURITY CLASSIFICATION OF THIS PAGE(When Data Entered)

Library Card

Civil Engineering Laboratory
VALIDATION OF SIMULATION TECHNIQUES FOR ELECTROMECHANICAL COUPLINGS IN ELECTRICAL MOTORS (Final), by K. T. Huang, Ph.D., and D. M. Shiroma
TN-1484 23 pp illus May 1977 Unclassified

1. Equivalent circuit 2. Single-phase induction motor I. Z-R000-01-142

High frequency injection and electromagnetic coupling techniques are used to measure the parameters of a single-phase induction motor to determine its equivalent circuit. This equivalent circuit is then programmed on the analog computer for verification. From the equivalent circuit, the electromechanical coupling which correlates the electrical and mechanical parameters can be determined. The analog simulation of the single-phase induction motor can then be used for experimentation, analysis, and design.

Unclassified

SECURITY CLASSIFICATION OF THIS PAGE(When Data Entered)

CONTENTS

INTRODUCTION

Electrical power systems include a large number of various types of power machinery. Of all the types of rotating machines in use today, the most common is the single-phase induction motor; therefore, it was picked as a representative electric motor for a series of tests at the Civil Engineering Laboratory (CEL). The objective of these tests is to look at the electromechanical coupling in the motor and obtain an analog simulation of the induction motor.

Electromagnetic coupling and high frequency signal injection can be used to accurately measure a system's electrical parameters such as currents and voltages without affecting its normal operating characteristics at 60 Hz. These measurement techniques are described in detail in a CEL Technical Note* and, thus, will be only briefly discussed in this report. It is sufficient to note that measurement techniques are much simpler for a motor, which is only a single-port network, than those for the two-port network described in Technical Note N-1473.

To determine the electromechanical coupling in the induction motor, both the electrical and mechanical parameters must be measured and the relationship linking these parameters determined.

The electrical properties of the single-phase induction motor are well-defined by its equivalent circuit. Measurements can be made in the high frequency range (800 Hz to 10K Hz) to determine the initial guess values of the equivalent circuit values. The speed of the motor is the main mechanical property that must be measured. This can then be used to calculate the slip, which is the quantity that determines the relationship between the electrical parameters and mechanical output for the induction motor. From determination of slip and initial guess values for the equivalent circuit, the induction motor can be programmed on the analog computer for laboratory analysis and experimentation.

High frequency signal injection and electromagnetic coupling measurement techniques can be used to measure the electrical properties of the motor, which provide the advantage of allowing measurements to be performed without any disturbance to the normal operation of the induction motor. Thus, the measurements and analog simulation may be accomplished with no disturbance to the operating electrical power system or loads.

---

* Civil Engineering Laboratory. Technical Note N-1473. Transfer immittance measurements of power elements, by K. T. Huang and D. M. Shiroma. Port Hueneme, CA 93043.

SINGLE-PHASE INDUCTION MOTOR

The single-phase induction motor consists primarily of a distributed stator winding and a squirrel-cage rotor. It is represented schematically in Figure 1. The AC supply voltage is applied to the single-phase stator winding which creates a magnetic field distribution that is stationary in space and pulsating in magnitude.

The stator winding is generally distributed in slots to produce a sinusoidal spatial flux distribution. The instantaneous spatial flux distribution can then be expressed as

$$\phi = \phi_1 \cos \theta \tag{1}$$

where θ is the angle between the stator coil axis and the particular position on the stator, and ϕ_1 is the instantaneous maximum in the flux distribution. Since the stator voltage and current are varying sinusoidally in time, ϕ_1 will also vary sinusoidally. Then

$$\phi_1 = \phi_{max} \cos \omega t \tag{2}$$

Combining Equations 1 and 2 gives:

$$\begin{aligned} \theta &= \phi_{max} \cos \omega t \cos \theta \\ &= \phi_{max} \left[\frac{1}{2} \cos(\theta + \omega t) + \frac{1}{2} \cos(\theta - \omega t)\right] \end{aligned} \tag{3}$$

Equation 3 indicates that the magnetic field distribution can be resolved into two rotating waves, a forward wave and a backward wave, which have the same magnitudes and synchronous speeds but which rotate in opposite directions.

Both of these waves produce induction motor action, and their effects are taken into account in the equivalent circuit of the single-phase induction motor shown in Figure 2. The top half of the circuit represents the effect of the forward wave, while the bottom half gives the effect of the backward wave. Both halves of the circuit are similar, differing only in the relationship with slip. In relation to the forward field, the relative speed between the field and the motor is

$$n_{sync} - n_{motor} = s\, n_{sync}$$

or equivalently

$$n_m = n_{sync}(1 - s)$$

where s = slip

n_{sync} = synchronous speed

n_m = speed of the machine

In relation to the backward field, however, the relative speed of the motor and the backward field is $n_{sync} + n_m$. In terms of previously defined quantities:

$$n_{sync} + n_m = n_{sync} + n_{sync}(1 - s) = n_{sync}(2 - s)$$

Thus, in the top half of the circuit we have r_2/s and in the bottom half we have $r_2/(2 - s)$. The factor of one-half is obtained from Equation 3, and represents the half-magnitude of the rotating stator waves.

The equivalent circuit contains five circuit parameters — r_1, r_2, x_1, x_2, and x_ϕ. Slip can be determined readily from measurements of motor speed and electrical frequency. Thus, to completely characterize the electromechanical coupling of the induction motor we must determine the five circuit parameters.

The nameplate of the single-phase induction motor used in the experiments contains the following data:

Westinghouse LifeLine T AC Motor 3 hp, single phase induction motor 1750 rpm, serial #7403 Model SLDP

EXPERIMENTAL SETUP AND MEASUREMENTS

The experimental setup is shown in Figure 3. The injection circuit consists of:

(1) Hewlett-Packard Audio Oscillator Model 201C, to supply the high frequency signal

(2) McIntosh 2100 Stereo Power Amplifier, to boost the high frequency signal before injecting it into the system

(3) A π-section filter and ferromagnetic core

The schematic of the injection circuit is illustrated in Figure 4. A sketch of a typical transfer function for the filter and core is shown in Figure 5. Two detection circuits are used, one to measure the high frequency current and the other to measure the high frequency voltage. The detection circuit, shown schematically in Figure 6, consists of:

(1) Hewlett-Packard wave analyzer Model 3581A to measure the particular high frequency injection signal

(2) A π-section filter and ferromagnetic core, similar to the ones used in the injection circuit

High frequency signals are induced into the system by electromagnetic induction, and the resulting high frequency voltage and currents are measured (again through electromagnetic induction). Measurements were taken in the high frequency range, 800 Hz to 10K Hz, and an additional measurement taken at 60 Hz under normal operating conditions of the motor. The graph of the magnitude of the induction motor's impedance, Z_{mag}, versus frequency is given in Figure 7. Also, the mechanical parameter (motor speed) was measured to determine slip. From these data, the initial guess values of the five unknown parameters in the equivalent circuit of the single-phase induction motor were determined.

SYNTHESIS OF EQUIVALENT CIRCUIT

To synthesize the equivalent circuit of the induction motor on the analog computer, initial guess values for the circuit parameters must first be determined. The method used in determining the initial guess values follows. Considering the case when slip is approximately 1, (this is valid for the high frequency range in which we are measuring) the equivalent circuit for the single-phase induction motor simplifies to the circuit shown in Figure 8. This can be further simplified by noting that at high frequencies $|x_\phi| >> |jx_2 + r_2|$ and can be considered an open circuit. Also $|x_2 + x_1| >> |r_1 + r_2|$, so the circuit reduces to a simple series circuit of x_1 and x_2. The inductance $(L_1 + L_2)$ can then be determined from the high frequency measurements. $Z_{mag} = \omega(L_1 + L_2)$ in the high frequency range, or $(L_1 + L_2) = Z_{mag}/\omega$. From the data in Figure 7, we obtain $L_1 + L_2 = 1.1$ mh. The initial guess values were picked with $L_1 = L_2$. Previous experiments on other power elements such as transformers had indicated this as a good approximation.

To determine r_2 and L_ϕ, we consider the case at 60 Hz when slip is small. With ω relatively small, $x_2/2$ and $r_2/[2(2 - s)]$ are small compared to the other elements. Also noting that r_1 and x_1 are also small while x_ϕ and r_2/s are large, the equivalent circuit now simplifies to that shown in Figure 9. The phasor diagram along with the basic equations of the circuit are illustrated in Figure 10. From measurements at 60 Hz, we have P = 3.5KW, V = 120v, I_1 = 41.2a, and n_m = 1753 rpm. From these measurements we calculate the power factor, the phase angle and the slip. These values are: pf = 0.71, θ = 44.9 degrees, and s = 0.0261.

Using the relationship given in Figure 10, we can now calculate the values for x_ϕ and r_2. These values are $x_\phi = 8.25\Omega$ and $r_2 = 0.21\Omega$. We also note that L_ϕ = 21.9 mh.

As an initial guess, r_1 was set equal to r_2, which appeared to be a good approximation as indicated by previous experiments conducted at CEL.

These initial guess values were then programmed into the Power System Simulator (PSS) analog computer and adjusted to provide the final analog simulation of the single-phase induction motor.

ANALOG PROGRAM TO OBTAIN CIRCUIT PARAMETERS

To simulate a power system or element on an analog computer, a circuit diagram that indicates all values of the circuit components is required. All connections on the analog computer will ultimately be based on the circuit diagram. The equivalent circuit of the single-phase induction motor is illustrated in a modified form in Figure 11. The circuit has been modified by the addition of "dummy" resistor r_d in parallel with the inductor $L_2/2$. This resistor has been added to simplify the analog simulation for obtaining the quantities $(V_4 - V_3)$ and V_5. The value of r_d ($r_d >> \omega L_2/2$) is such that it will have little effect on the circuit. Its nominal value is 240Ω.

Using the circuit diagram as a guide, a signal flow diagram is now developed. The signal flow diagram represents the hardware implementation required in programming the Power System simulator. It is designed to have a minimum number of modules to simplify the wiring of the analog computer and arranged to provide ease of adjustment of the circuit values. The signal flow diagram for the induction motor is shown in Figure 12. The signals present at various points in the circuit are indicated.

The final instrumentation (of the single-phase induction motor) on the analog computer is illustrated in Figure 13. This diagram shows the actual modules used and the interconnections between them. It also gives the various signals present in the circuit and accounts for the 180-degree phase shift through most of the modules. The input signals are: an AC voltage waveform designated V_1, a constant -2 Vdc, and a variable dc voltage S_ℓ, representing the slip. The output signal is the AC current I_1.

With the PSS thus wired, and the circuit elements tuned to their initial guess values, input signals; V_1, S_ℓ, and -2 Vdc, are fed in and output I_1 is monitored. The circuit elements are then adjusted to provide the same I_1 for a given V_1 as was measured by electromagnetic coupling techniques and high frequency injection. After these adjustments have been made, the induction motor can be considered as analogically synthesized.

HIGH FREQUENCY CHARACTERISTICS USING POWER SYSTEM SIMULATOR

Having analogically synthesized the single-phase induction motor, it remains to verify the high frequency response of the circuit. The PSS, however, is designed to operate at a center frequency of 60 Hz with a nominal range of 6 Hz to 600 Hz. Simulation of high frequencies beyond 600 Hz will result in decreased accuracy. To obtain results in the 800 Hz to 10K Hz range, frequency scaling techniques must be used.

For frequency scaling, the high frequency source is replaced with a source whose frequency falls within the nominal range of the PSS. Then all values of inductances, and capacitances are modified by some frequency scaling factor, as indicated by Equations 4 and 5.

$$L_o \omega_o = \left(L_o f_N\right)\left[2\pi\left(\frac{f_o}{f_N}\right)\right] = L \omega \qquad (4)$$

$$\frac{1}{C_o \omega_o} = \frac{1}{(C_o \omega_N) \frac{\omega_o}{\omega_N}} = \frac{1}{(C_o f_N)\left[2\pi\left(\frac{f_o}{f_N}\right)\right]} = \frac{1}{C \omega} \qquad (5)$$

where f_o = the original high frequency

f_N = frequency scaling factor

$\omega_o = 2 \pi f_o$

$\omega_N = 2 \pi f_N$

$\omega = 2 \pi f$

$f = f_o/f_N$ = scaled frequency (between 6 Hz and 60 Hz)

L_o = original inductance

L = scaled inductance

C_o = original capacitance

C = scaled capacitance

The time response is then

$$t = f_N t_o \qquad (6)$$

where t_o = original response time

t = scaled response time

The circuit response for the original high frequency signal can thus be determined from the scaled frequency response. The results of the analog program is plotted in Figure 14, along with experimentally obtained high frequency measurements. The simulated circuit results correlate closely with experimentally determined data.

ANALOG SIMULATION AT 60 HZ

Having obtained successful correlation of high frequency measurements, analog simulation using CEL Power System Simulator was performed at 60 Hz, with varying values of slip. This data was then compared with experimentally obtained measurements on the single-phase induction motor operating at 60 Hz with different mechanical loads. The graphs in Figure 15 are plots of Z versus slip, where Z is the magnitude of the impedance V_{in}/I_{in}. The close correlation between the two graphs verifies the accuracy of the synthesized equivalent circuit.

ELECTROMAGNETIC COUPLING

With the equivalent circuit of the single-phase induction motor completed, the mechanical output power can now be calculated. Thus the electromechanical coupling — that is, the correlation between the electrical input parameters (voltage and current) and the mechanical output parameters (torque and power) — can be determined.

The equivalent circuit of the induction motor in Figure 2 can be simplified by lumping various impedances to obtain the circuit shown in Figure 16. Here, the circuit is composed of an impedance $\bar{Z}_f$, which accounts for the effects of the forward field, and a $\bar{Z}_b$, which considers the effect of the backward field. $\bar{Z}_f$ is the parallel combination of $x_\phi/2$ and the series $r_2/2s$ and $x_2/2$ branch, while $\bar{Z}_b$ is the parallel combination of $x_\phi/2$ and the series $r_2/[2(2 - s)]$ and $x_2/2$ branch. The basic relationships are as follows:

$$\bar{Z}_f = R_f + j\,x_f \tag{7}$$

$$\bar{Z}_b = R_b + j\,x_b \tag{8}$$

$$I_m = \frac{V_{in}}{Z_{mag}} \tag{9}$$

where

$$R_f = \frac{1}{2}\left[\frac{\frac{r_2}{S}\,x_\phi^2}{\left(\frac{r_2}{S}\right)^2 + (x_2 + x_\phi)^2}\right]$$

$$x_f = \frac{1}{2}\left\{\frac{x_\phi\left[\left(\frac{r_2}{S}\right)^2 + x_2(x_2 + x_\phi)\right]}{\left(\frac{r_2}{S}\right)^2 + (x_2 + x_\phi)^2}\right\}$$

$$R_b = \frac{1}{2}\left[\frac{\frac{r_2}{(2 - S)}\,x_\phi^2}{\left(\frac{r_2}{2 - S}\right)^2 + (x_2 + x_\phi)^2}\right]$$

$$x_b = \frac{1}{2}\left\{\frac{x_\phi\left[\left(\frac{r_2}{2 - S}\right)^2 + x_2(x_2 + x_\phi)\right]}{\left(\frac{r_2}{2 - S}\right)^2 + (x_2 + x_\phi)^2}\right\}$$

Then,

$$\overline{Z}_{mag} = r_1 + j\,x_1 + \overline{Z}_f + \overline{Z}_b = Z_R + j\,Z_I$$

Z_R is the real component of $\overline{Z}_{mag}$ and Z_I is the imaginary component.

The power that is delivered to the forward field is then $P_f = I_m^2 R_f$, and the power to the backward field is $P_b = I_m^2 R_b$. The related, internally induced torques are $T_f = P_f/\omega_S$ and $T_b = P_b/\omega_S$, respectively, where ω_S is the synchronous angular velocity expressed in mechanical radians per second.

The net torque T is due to the effect from the forward and backward fields. Since these fields rotate in opposite directions, $T = T_f - T_b = (1/\omega_S)(P_f - P_b)$. Then output mechanical power P_{mech} is:

$$P_{mech} = \omega_{mech}\,T = (1 - S)\,\omega_S\,T = (1 - S)(P_f - P_b)$$

$$= (1 - S)\,I_m^2\,(R_f - R_b) = (1 - S)\,V_{in}^2\,\frac{R_f - R_b}{Z_R^2 - Z_I^2} \qquad (10)$$

Using Equation 10, we can determine the mechanical output for any input voltage and any given slip. From measurement of voltage and speed, all electrical and mechanical parameters of the single-phase induction motor can be determined.

CONCLUSION

The high frequency measurement range used in the experiments was 800 Hz to 10K Hz. The lower end of the range was limited by the actual filter circuit used. For more accurate synthesis of the single-phase induction motor, measurements should be made at the lowest frequencies possible. This will be limited by the noise level at frequencies closer to 60 Hz. Measurements at frequencies which are harmonics of 60 Hz should be avoided as they tend to be erroneous.

High frequency injection and electromagnetic coupling measurement techniques can provide data which can be used with the analog computer to obtain accurate synthesis of the equivalent circuit of the induction motor. These measurements can be made with almost no effect on the normal operation of the induction motor.

The CEL Power System Simulator is a valuable tool in analysis, experimentation, and design. Both mechanical and electrical characteristics can be predicted for various loads and sources on the induction motor. Thus experimentation and analysis of effects of the induction motor on a power system can be done on the simulator instead of the actual power system. Also, various protective devices such as circuit breakers, fuses, etc., can be designed from analysis of various faults on the induction motor, such as locked rotor or shorted windings. These faults could result in excessively high currents and cannot be performed on an operating system, but could be easily simulated.

BIBLIOGRAPHY

A. E. Fitzgerald and Charles Kingsley, Jr. Electric machinery. New York, NY, McGraw-Hill Book Company, 1961.

V. Del Toro. Electromechanical devices for energy conversion and control systems. Englewood Cliffs, NJ, Prentice-Hall, Inc., 1968.

A. S. Jackson. Analog computation. New York, NY, McGraw-Hill Book Company, Inc., 1960.

C. L. Johnson. Analog computer techniques. New York, NY, McGraw-Hill Book Company, Inc., 1963.

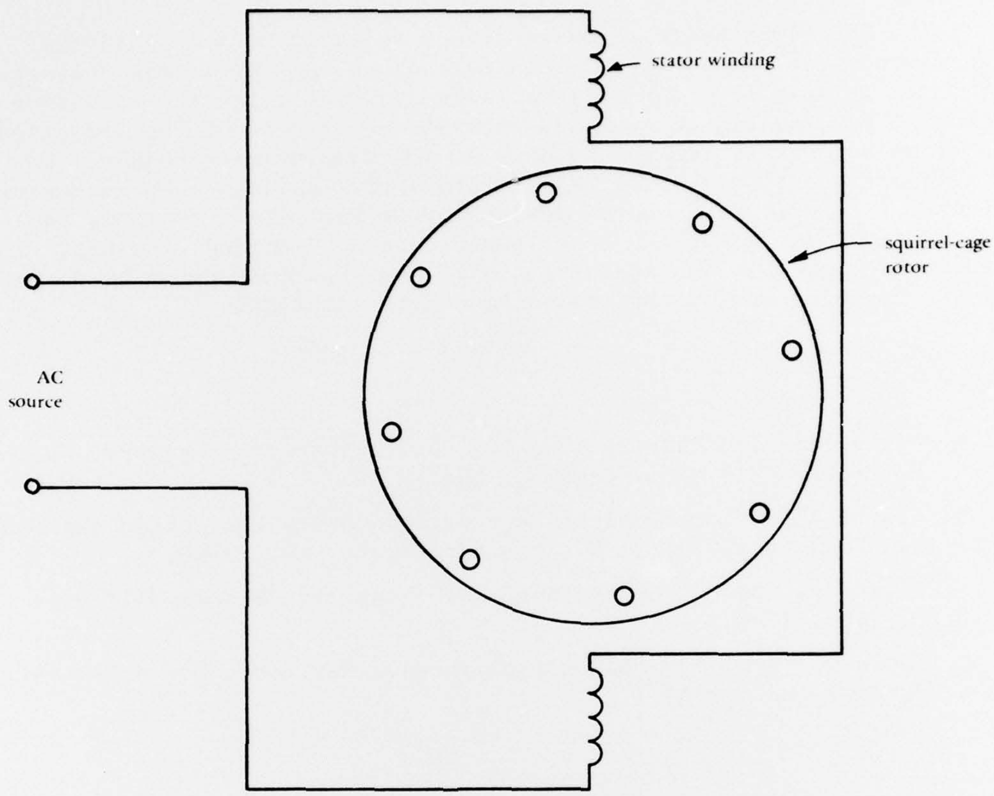

Figure 1. Single-phase induction motor.

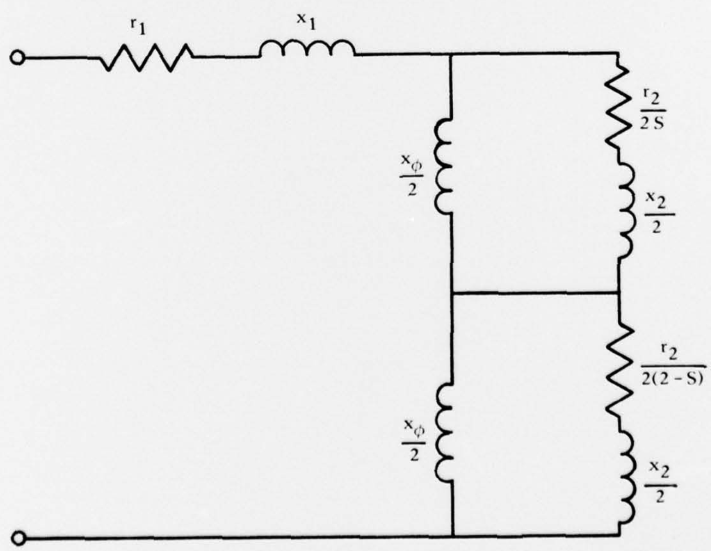

Figure 2. Equivalent circuit of single-phase induction motor.

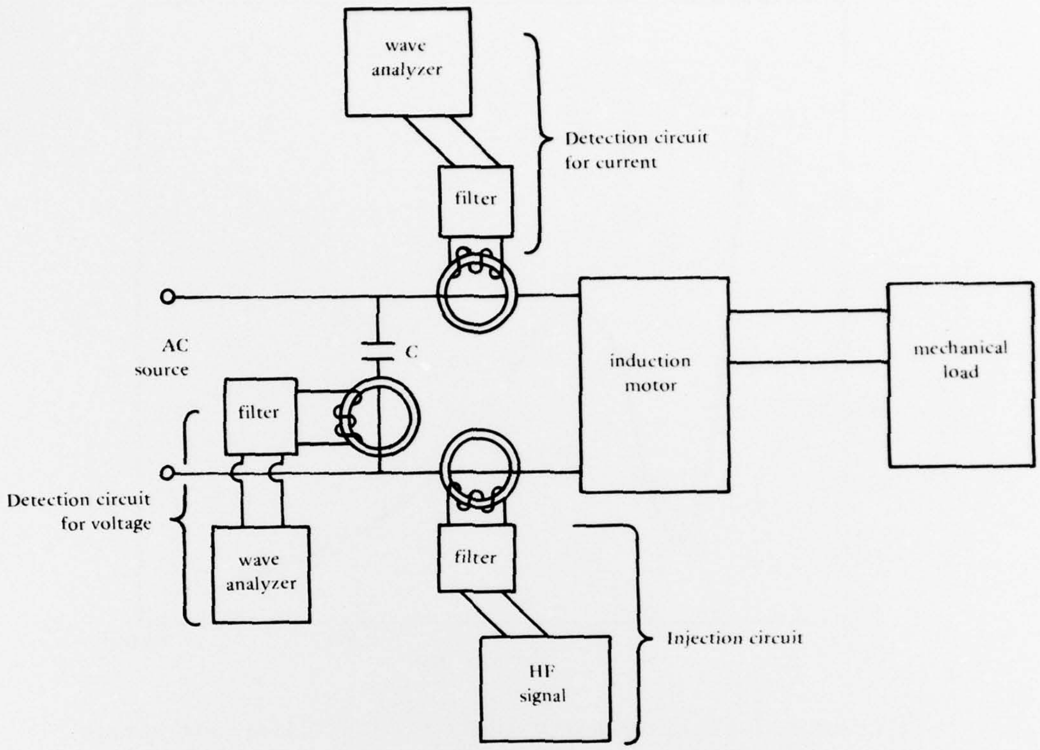

Figure 3. Test setup.

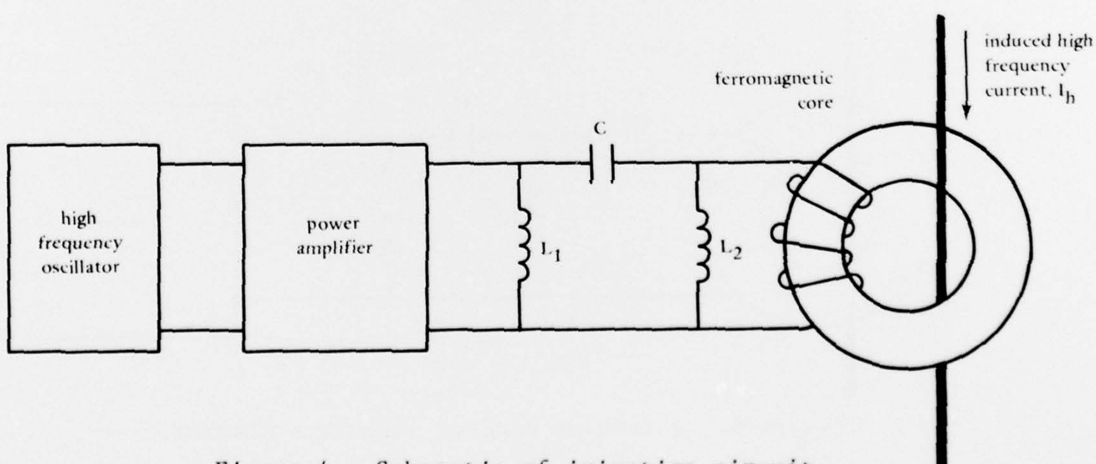

Figure 4. Schematic of injection circuit.

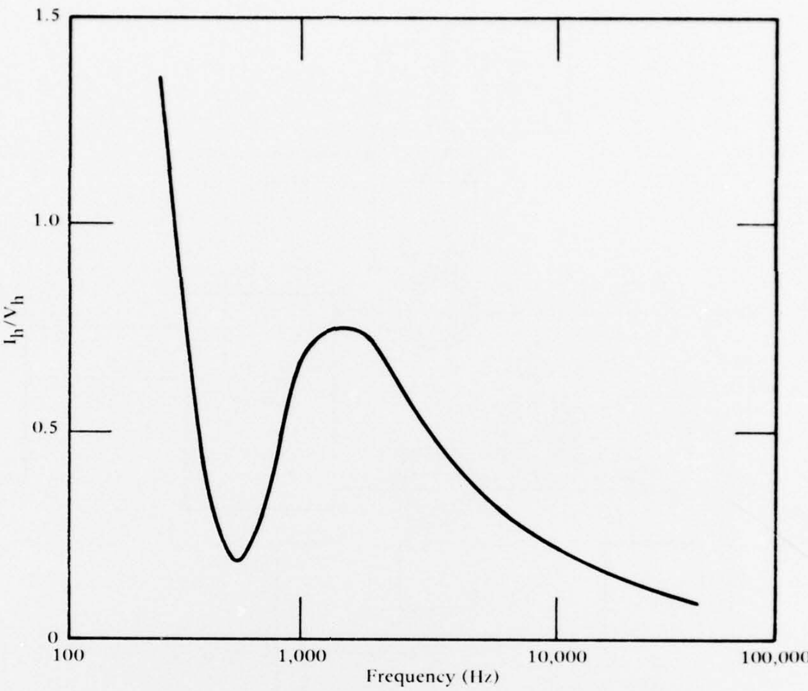

Figure 5. Typical transfer function for filter and core.

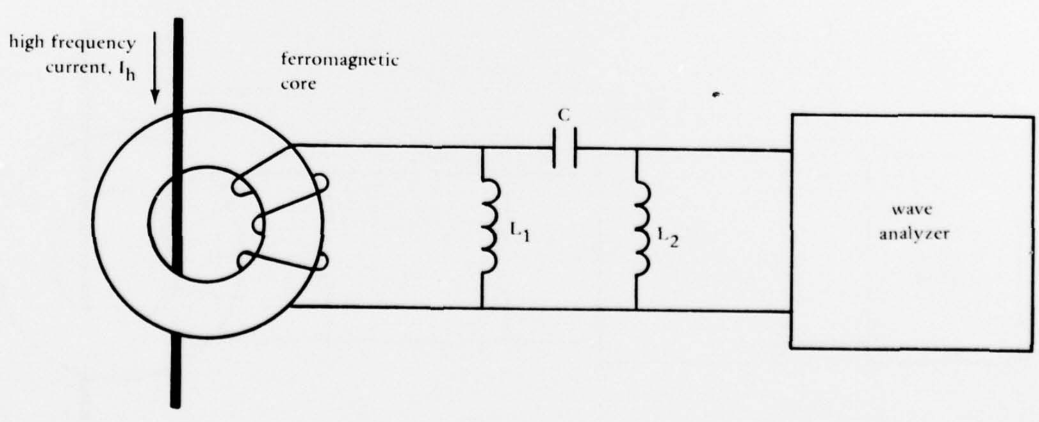

Figure 6. Detection circuit schematic diagram.

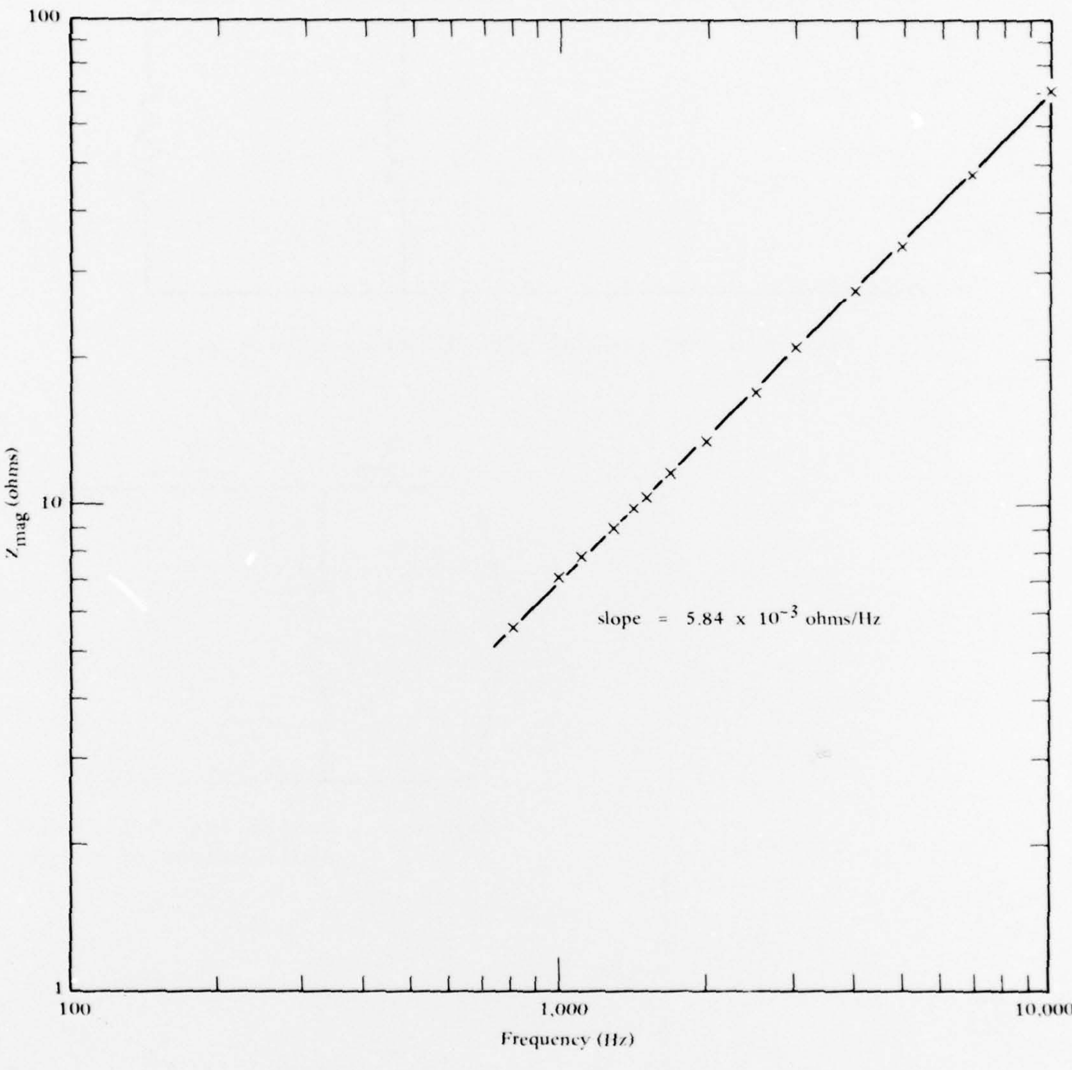

Figure 7. Plot of magnitude of motor impedance versus frequency.

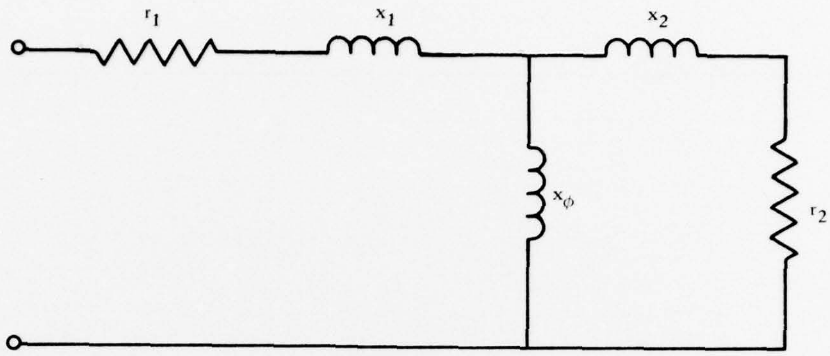

Figure 8. Equivalent circuit where slip = 1.

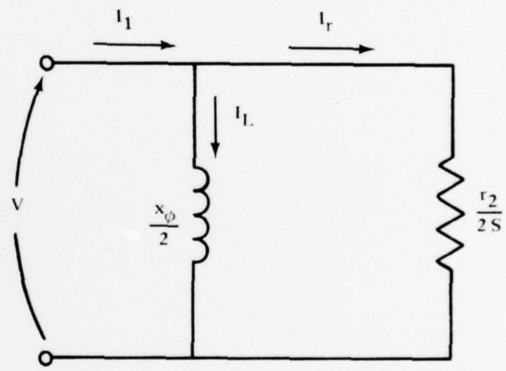

Figure 9. Equivalent circuit for small values of slip.

$$I_r = \frac{V}{\left(\frac{r_2}{S}\right)}$$

$$I_L = \frac{V}{\left(\frac{x_\phi}{2}\right)}$$

$$\tan\theta = \frac{\left(\frac{r_2}{S}\right)}{x_\phi}$$

$$I_r = I\cos\theta$$

$$I_L = I\sin\theta$$

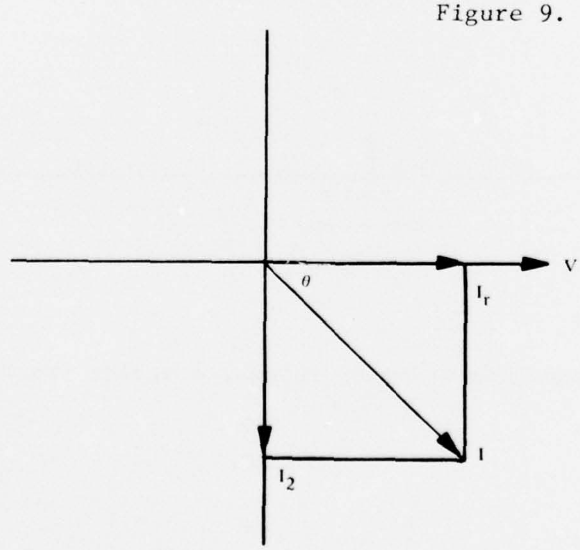

Figure 10. Phasor diagram of simplified equivalent circuit.

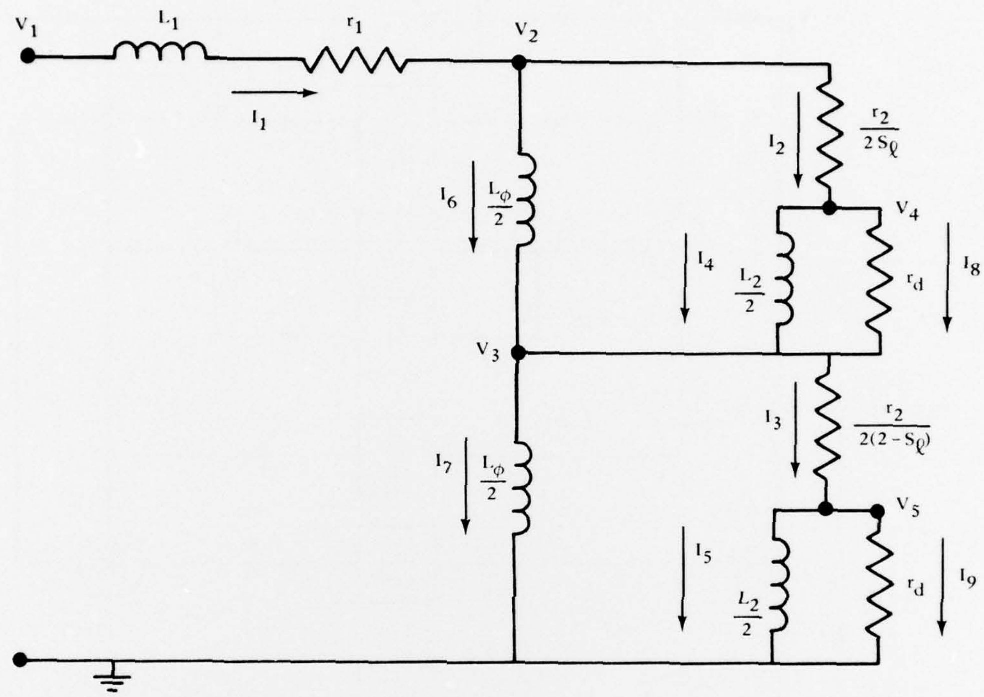

Figure 11. Modified circuit for analog program.

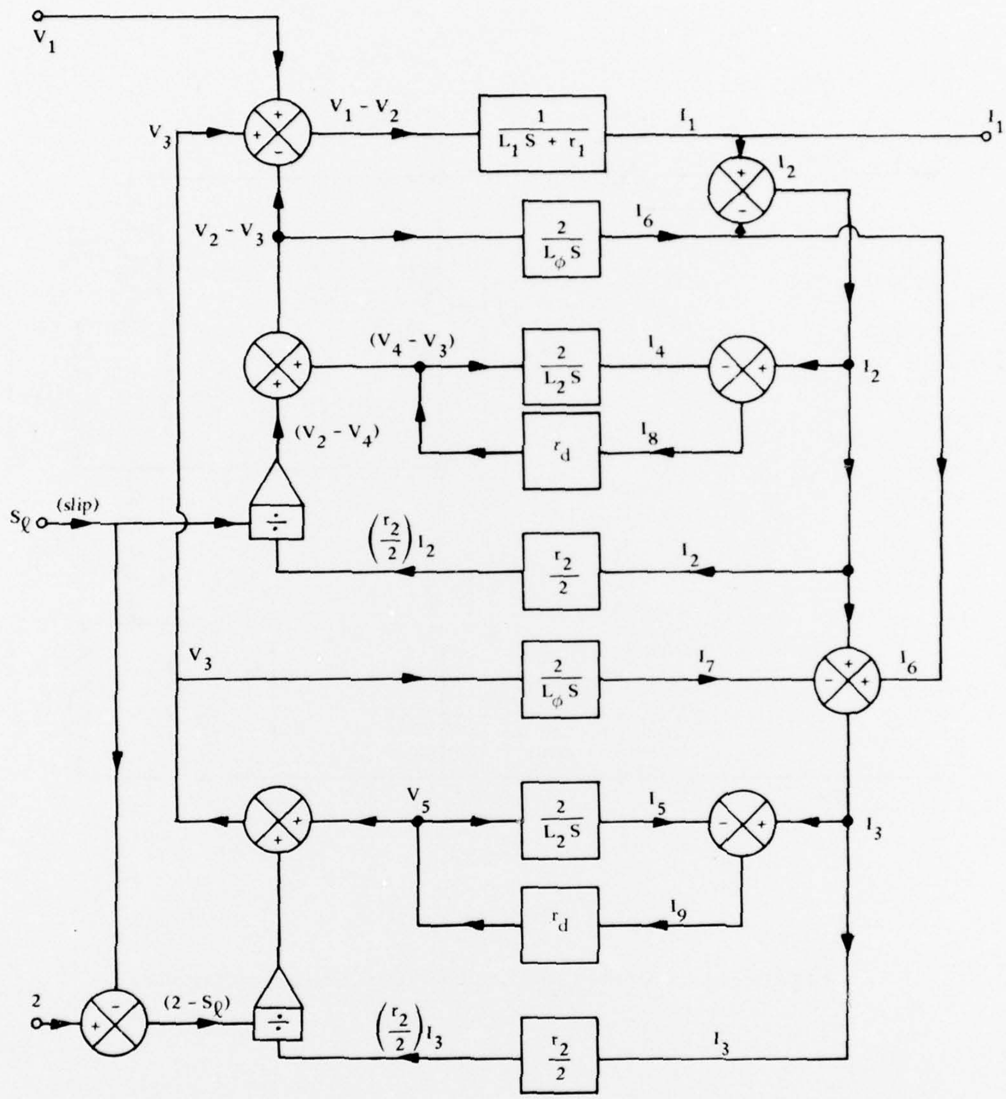

Figure 12. Signal flow diagram.

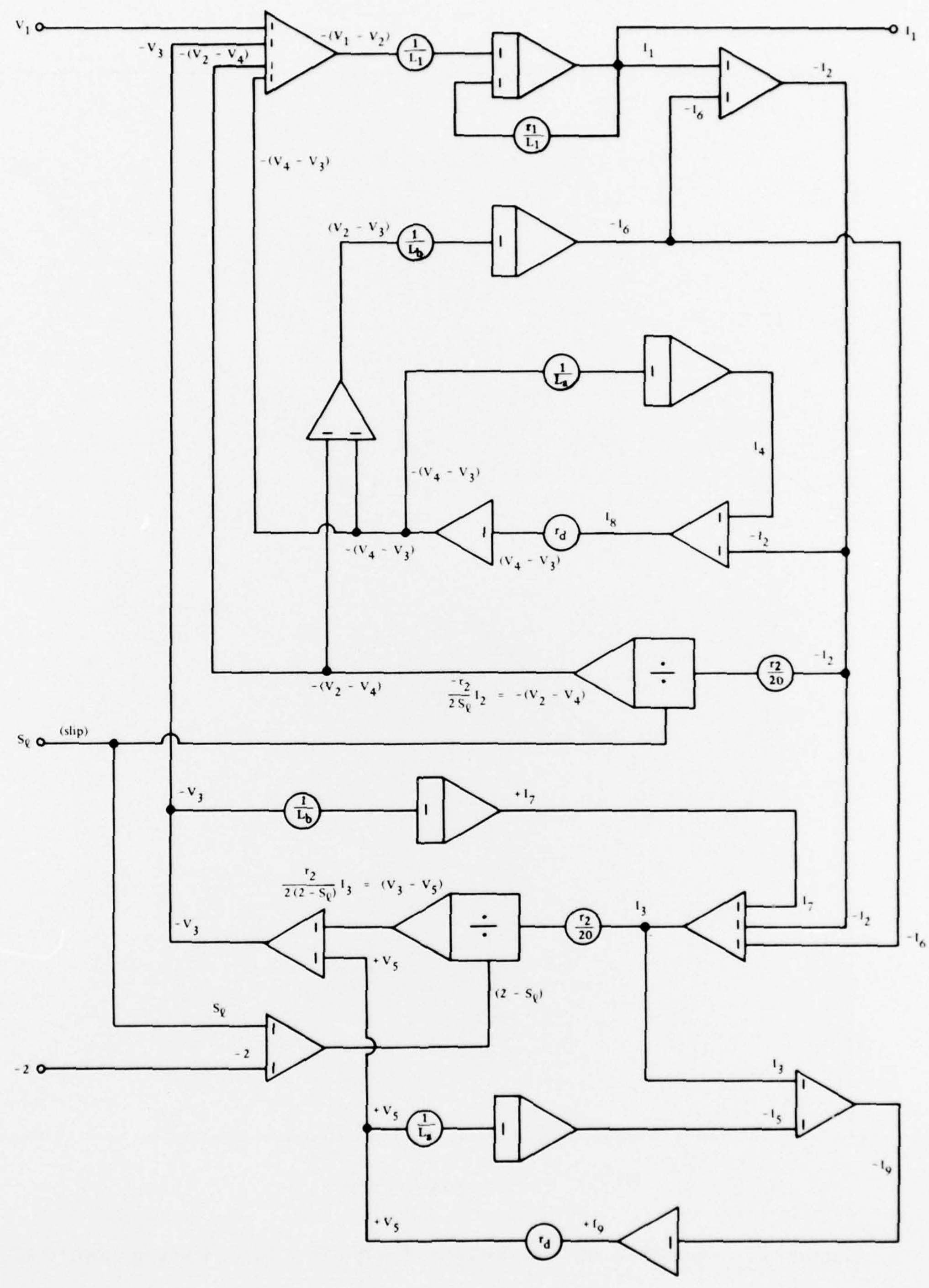

Figure 13. Instrumentation for analog simulation of induction motor.

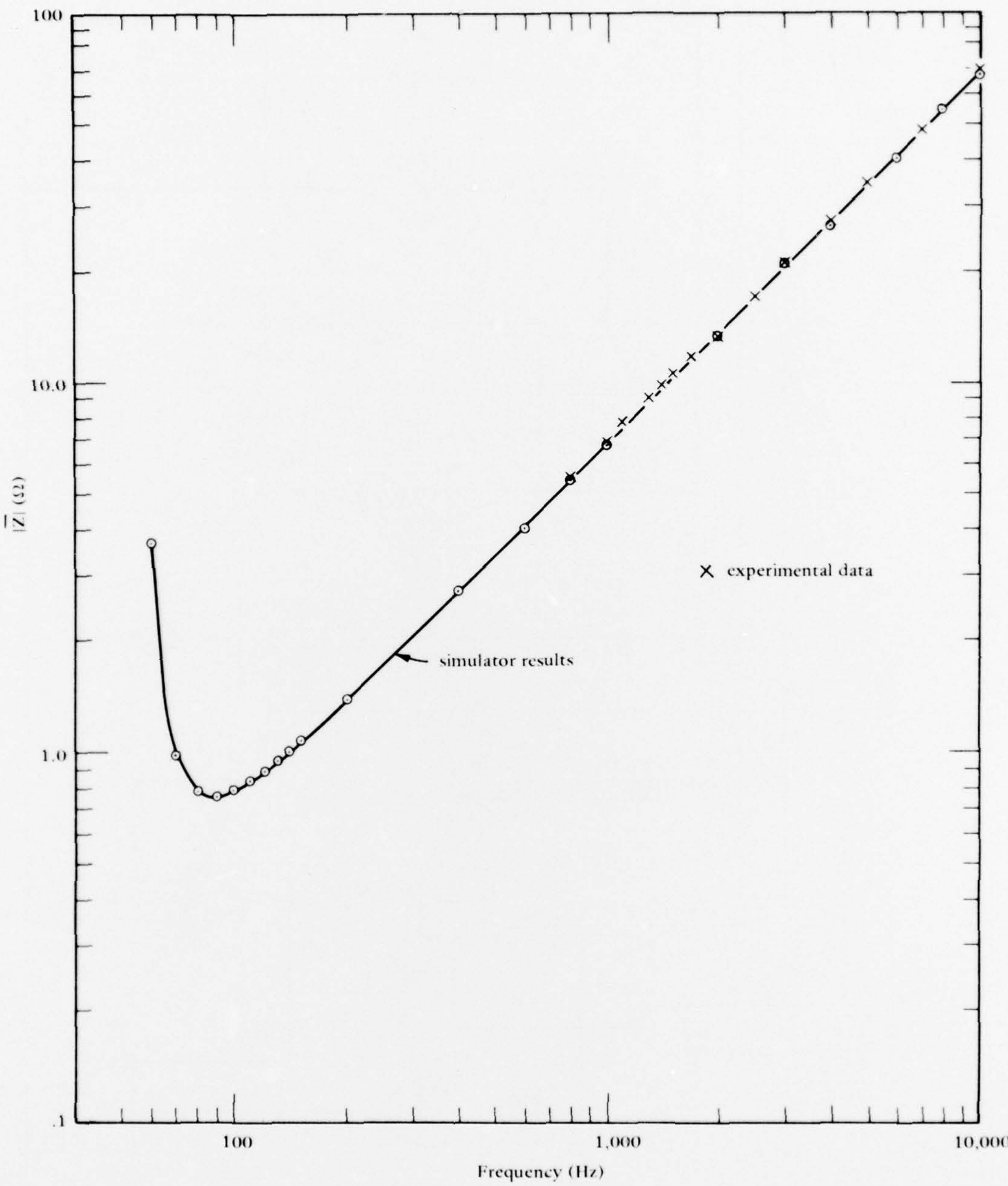

Figure 14. Results of $|\overline{Z}|$ versus frequency from analog computer.

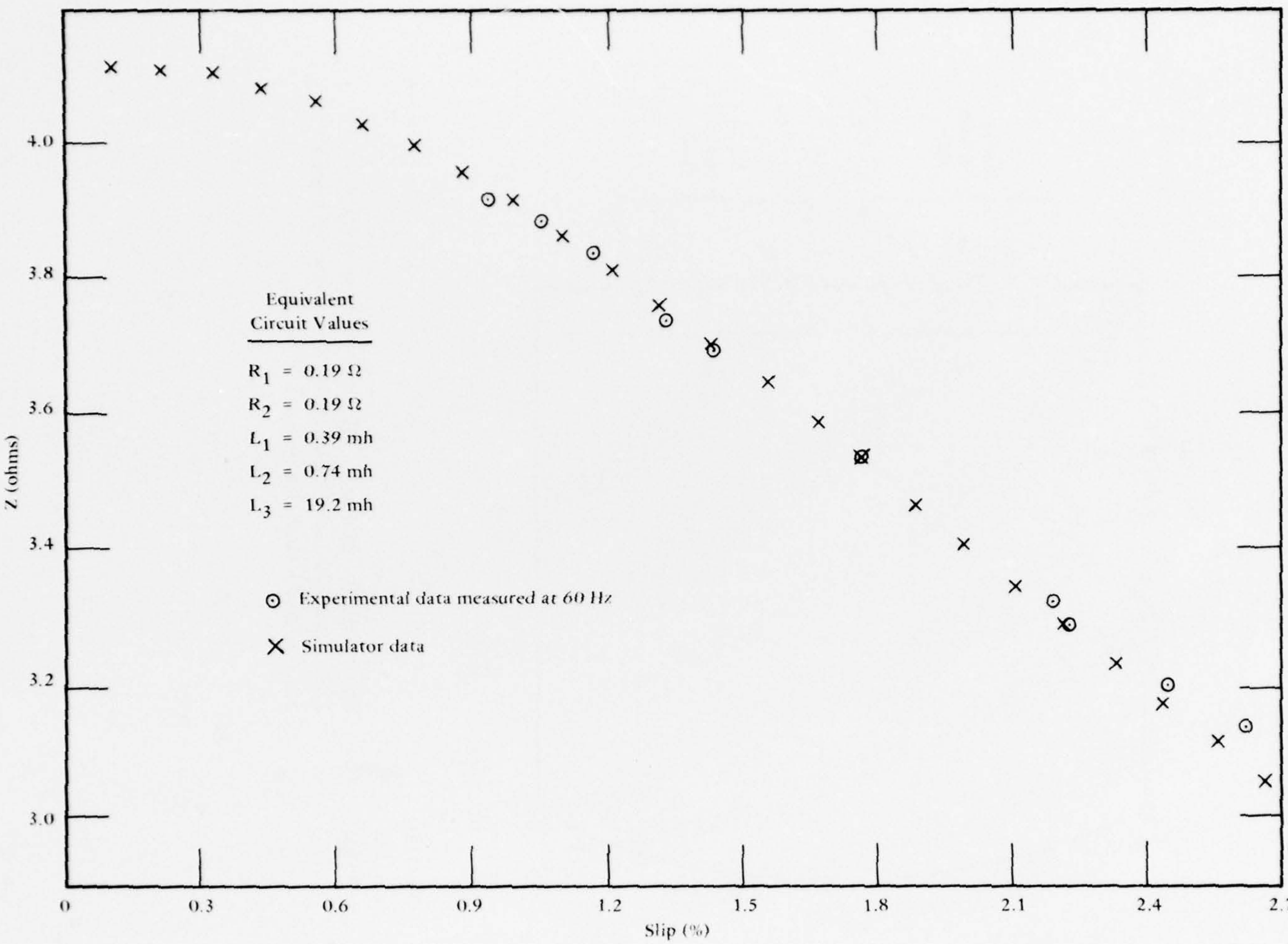

Figure 15. Z_{mag} versus slip, comparing experimental data and simulated data.

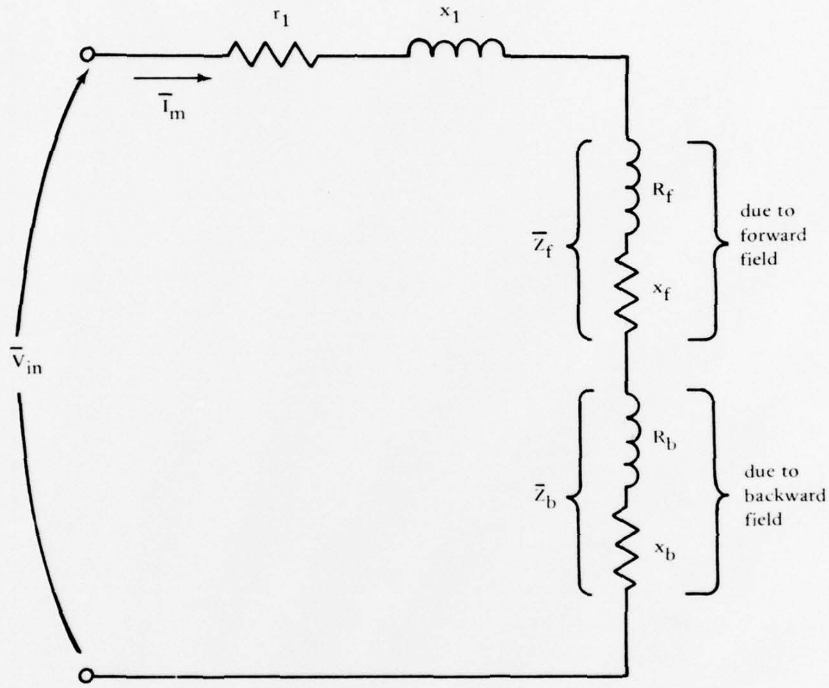

Figure 16. Equivalent circuit of induction motor with impedances combined to show effects of forward and backward fields.

DISTRIBUTION LIST

AFB AFCEC/XR, Tyndall FL; CESCH, Wright-Patterson; HQ Tactical Air Cmd (R. E. Fisher), Langley AFB VA; SAMSO/DEB, Norton AFB CA; Stinfo Library, Offutt NE
ARMY AMSEL-GG-TD, Fort Monmouth NJ; BMDSC-RE (H. McClellan) Huntsville AL; DAEN-CWE-M (LT C D Binning), Washington DC; DAEN-FEU, Washington DC; Tech. Ref. Div., Fort Huachuca, AZ
ARMY BALLISTIC RSCH LABS AMXBR-XA-LB, Aberdeen Proving Ground MD
ARMY CORPS OF ENGINEERS Seattle Dist. Library, Seattle WA
ARMY ENVIRON. HYGIENE AGCY Water Qual Div (Doner), Aberdeen Prov Ground, MD
ASST SECRETARY OF THE NAVY Spec. Assist Energy (P. Waterman), Washington DC
BUMED Code 41-1 (CDR Nichols)
BUREAU OF RECLAMATION Code 1512 (C. Selander) Denver CO
MCB ENS S.D. Keisling, Quantico VA
CNO Code NOP-964, Washington DC
COMFLEACT, OKINAWA PWO, Kadena, Japan
COMNAVMARIANAS Code N4, Guam
DEFENSE DOCUMENTATION CTR Alexandria, VA
DTNSRDC Code 42, Bethesda MD
ENERGY R&D ADMIN. Dr. Cohen; Dr. Vanderryn, Washington DC
FLTCOMBATDIRSYSTRACENLANT PWO, Virginia Bch VA
KWAJALEIN MISRAN BMDSC-RKL-C
MARINE CORPS BASE Code 43-260, Camp Lejeune NC; M & R Division, Camp Lejeune NC; Maint. Office, Camp Pendleton CA; PWO, Camp S. D. Butler, Kawasaki Japan
MARINE CORPS HQS Code LFF-2, Washington DC
MCAS Code PWE, Kaneohe Bay HI; Code S4, Quantico VA; PWD, Dir. Maint. Control Div., Iwakuni Japan; PWO, Yuma AS
MCB Base Maint. Offr, Quantico VA
MCRD PWO, San Diego Ca
NAD Code 011B-1, Hawthorne NV
NAS PWO., Moffett Field CA; ROICC Off (J. Sheppard), Point Mugu CA; SCE, Barbers Point HI
NATPARACHUTETESTRAN PW Engr, El Centro CA
NAVCOMMAREAMSTRSTA Code W-602, Honolulu, Wahiawa HI; PWO, Wahiawa HI
NAVCOMMSTA PWO, Adak AK
NAVFACENGCOM Code 2014 (Mr. Taam), Pearl Harbor HI
NAVREGMEDCEN SCE (LCDR B. E. Thurston), San Diego CA; SCE, Guam
NAVSCOLCECOFF C35
NAVSECGRUACT PWO, Torri Sta, Okinawa
NAVSHIPYD Code 400, Puget Sound; Code 410, Mare Is., Vallejo CA; PWO, Mare Is.; PWO, Puget Sound; SCE, Pearl Harbor HI
NAVSTA PWD (L. Ross), Midway Island; PWO; SCE, San Diego CA; SCE, Subic Bay, R.P.
NAVSUPPACT CO, Seattle WA; Code 4, 12 Marine Corps Dist, Treasure Is., San Francisco CA
NAD Engr. Dir; PWD Nat./Resr. Mgr Forester, McAlester OK
NAF PWO Sigonella Sicily
NAS Asst C/S CE; Code 187, Jacksonville FL; Code 70, Atlanta, Marietta GA; Dir. Util. Div., Bermuda; PWC Code 40 (C. Kolton); PWD Maint. Div., New Orleans, Belle Chasse LA; PWD, Willow Grove PA; PWO; PWO; PWO Chase Field; PWO Whiting Fld, Milton FL; PWO, Kingsville TX; PWO, Millington TN; R. Kline; SCE Lant Fleet
NATNAVMEDCEN PWO
NAVAL FACILITY PWO, Cape Hatteras, Buxton NC; PWO, Centerville Bch, Ferndale CA; PWO, Guam; PWO, Lewes DE
NAVCOASTSYSLAB Code 423 (D. Good), Panama City FL; Code 710.5 (J. Quirk); Library
NAVCOMMSTA CO (61E); PWO, Fort Amador Canal Zone
NAVCOMMUNIT Cutler/E. Machias ME (PW Gen. For.)
NAVFACENGCOM Code 0433B; Code 0451; Code 04B3; Code 04B5; Code 101; LANTDIV (J.L. Dettbarn) Norfolk, VA.; Code 1023 (M. Carr); Code 104
NAVFACENGCOM - SOUTH DIV. Code 90, RDT&ELO, Charleston SC
NAVHOSP LT R. Elsbernd, Puerto Rico
NAVORDSTA PWO, Louisville KY
NAVRADRECFAC PWO, Kami Seya Japan
NAVREGMEDCEN PWO; PWO Newport RI

NAVSECGRUACT PWO, Edzell Scotland; PWO, Puerto Rico
NAVSHIPYD Code 440, Norfolk; Code 450, Charleston SC; Library, Portsmouth NH;
NAVSTA CO; CO; Engr. Dir., Rota Spain; Maint. Cont. Div., Guantanamo Bay Cuba; Maint. Div. Dir/Code 531, Rodman Canal Zone; PWO, Keflavik Iceland; PWO, Puerto Rico; ROICC, Rota Spain
NAVSUPPACT Plan/Engr Div., Naples Italy
NAVSURFWPNCEN PWO, White Oak, Silver Spring, MD
NAVWPNCEN PWO (Code 70), China Lake CA
NAVWPNSTA Maint. Control Dir., Yorktown VA; PWO
NAS CO, Guantanamo Bay Cuba; Code 114, Alameda CA; Code 18700, Brunswick ME; Code 18E (ENS P.J. Hickey), Corpus Christi TX; PWD (M.B. Trewitt), Dallas TX; PWD, Maintenance Control Dir., Bermuda
NATL RESEARCH COUNCIL Naval Studies Board, Washington DC
NAVACT PWO, London UK
NAVAVIONICFAC PWD Deputy Dir. D/701, Indianapolis, IN
NAVBASE Code 111 (A. Castronovo), Philadelphia PA
NAVCOMMSTA PWO, Norfolk VA
NAVCONSTRACEN CO (CDR C.L. Neugent), Port Hueneme, CA
NAVFACENGCOM - CHES DIV. Code 101; Code 402 (R. Morony); Code 403 (H. DeVoe)
NAVFACENGCOM - LANT DIV. RDT&ELO 09P2, Norfolk VA
NAVFACENGCOM - NORTH DIV. (Boretsky); Code 1028, RDT&ELO, Philadelphia PA; Code 114 (A. Rhoads); Design Div. (R. Masino), Philadelphia PA; ROICC, Contracts, Crane IN
NAVFACENGCOM - PAC DIV. Code 402, RDT&E, Pearl Harbor HI; Commanders
NAVFACENGCOM - SOUTH DIV. Dir., New Orleans LA
NAVFACENGCOM - WEST DIV. 102; 112; AROICC, Contracts, Twentynine Palms CA; AROICC, Point Mugu CA; Codes 09PA; O9P/20
NAVFACENGCOM CONTRACTS Bethesda, Design Div. (R. Lowe) Alexandria VA; Dir, Eng. Div., Exmouth, Australia; Eng Div dir, Southwest Pac, PI; OICC/ROICC, Balboa Canal Zone; ROICC, Pacific, San Bruno CA; TRIDENT (CDR J.R. Jacobsen), Bremerton WA 98310
NAVFORCARIB Commander (N42), Puerto Rico
NAVMARCORESTRANCEN ORU 1118 (Cdr D.R. Lawson), Denver CO
NAVNUPWRU MUSE DET OIC, Port Hueneme CA
NAVOCEANSYSCEN Code 65 (H. Talkington); Code 6565 (Tech. Lib.), San Diego CA; Code 6700; Code 7511 (PWO)
NAVPETOFF Code 30, Alexandria VA
NAVSCOLCECOFF CO, Code C44A
NAVSHIPYD CO Marine Barracks, Norfolk, Portsmouth VA; Code 202.4, Long Beach CA; Code 202.5 (Library) Puget Sound, Bremerton WA; Code 453 (H. Clements), Vallejo CA; Code 453 (Util. Supr), Vallejo CA; Code Portsmouth NH; PWD (Code 400), Philadelphia PA; PWD (LT N.B. Hall), Long Beach CA
NAVSTA PWD (LT W.H. Rigby), Guantanamo Bay Cuba; Utilities Engr Off. (LTJG A.S. Ritchie), Rota Spain
NAVSUBASE SCE, Pearl Harbor HI
NAVSUPPACT AROICC (LT R.G. Hocker), Naples Italy; CO, Brooklyn NY
NAVTRAEQUIPCEN Technical Library, Orlando FL
NAVWPNCEN ROICC (Code 702), China Lake CA
NAVWPNSTA Code 092A (C. Fredericks) Seal Beach CA; ENS G.A. Lowry, Fallbrook CA
NAVFACENGCOM - WEST DIV. Code 04B
NAVOCEANSYSCEN SCE (Code 6600), San Diego CA
NAVSHIPRANDCEN (LCDR Dieterle), Carderock Lab., Bethesda, MD
NAVSHIPYD Code 420, Maint. Control, Long Beach, CA
NAVWPNSUPPCEN PWO
NAVEDTRAPRODEVCEN Tech. Library
NAVFACENGCOM - LANT DIV. Eur. BR Deputy Dir, Naples Italy
NAVSUBASE ENS S. Dove, Groton, CT; LTJG D.W. Peck, Groton, CT
NCBC CEL (CAPT N. W. Petersen), Port Hueneme, CA; CEL AOIC; Code 10; Code 400, Gulfport MS; PW Engrg, Gulfport MS; PWO (Code 80); PWO, Davisville RI
NCBU 411 OIC, Norfolk VA
NCR 20, Commander
NMCB 5, Operations Dept.; Forty, CO; THREE, Operations Off.
NROTCU Univ Colorado (LT D R Burns), Boulder CO
NSC E. Wynne, Norfolk VA
NTC Commander; SCE
NUSC Code EA123 (R.S. Munn), New London CT
OCEANSYSLANT LT A.R. Giancola, Norfolk VA

OFFICE SECRETARY OF DEFENSE OASD (I&L) Pentagon (T. Casberg), Washington DC
ONR Code 484, Arlington VA
PMTC Pat. Counsel, Point Mugu CA
PWC ENS J.E. Surash, Pearl Harbor HI; ACE Office (LTJG St. Germain); Code 116 (ENS A. Eckhart); Code 120, Oakland CA; Code 120C (A. Adams); Code 200, Great Lakes IL; Code 200, Oakland CA; Code 220; Code 505A (H. Wheeler); OIC CBU-405, San Diego CA; XO
SPCC PWO (Code 120 & 122B) Mechanicsburg PA
USCG (G-ECV/61) (Burkhart) Washington, DC; HQ (GECV-3), Washington DC
USCG ACADEMY LT N. Stramandi, New London CT
USNA Ch. Mech. Engr. Dept; PWD Engr. Div. (C. Bradford)
WPNSTA EARLE Code 092, Colts Neck NJ
COLORADO STATE UNIV., FOOTHILL CAMPUS Engr Sci. Branch, Lib., Fort Collins CO
CORNELL UNIVERSITY Ithaca NY (Serials Dept, Engr Lib.)
DAMES & MOORE LIBRARY LOS ANGELES, CA
ILLINOIS STATE GEO. SURVEY Urbana IL
LEHIGH UNIVERSITY Bethlehem PA (Linderman Lib. No.30, Flecksteiner)
LIBRARY OF CONGRESS WASHINGTON, DC (SCIENCES & TECH DIV)
MASSACHUSETTS INST. OF TECHNOLOGY Cambridge MA (Rm 10-500, Tech. Reports, Engr. Lib.); Cambridge MA (Rm 14 E210, Tech. Report Lib.)
NY CITY COMMUNITY COLLEGE BROOKLYN, NY (LIBRARY)
PURDUE UNIVERSITY Lafayette, IN (CE LIB)
UNIVERSITY OF CALIFORNIA BERKELEY, CA (OFF. BUS. AND FINANCE, SAUNDERS)
UNIVERSITY OF DELAWARE Newark, DE (Dept of Civil Engineering, Chesson)
UNIVERSITY OF ILLINOIS URBANA, IL (LIBRARY)
UNIVERSITY OF NEBRASKA-LINCOLN LINCOLN, NE (SPLETTSTOESSER)
UNIVERSITY OF CALIFORNIA Berkeley CA (E. Pearson)
UNIVERSITY OF MASSACHUSETTS (Heronemus), Amherst MA CE Dept
UNIVERSITY OF TEXAS Inst. Marina Sci (Library), Port Aransas TX
UNIVERSITY OF WISCONSIN Milwaukee WI (Ctr of Great Lakes Studies)
URS RESEARCH CO. LIBRARY SAN MATEO, CA
US DEPT OF COMMERCE NOAA, Pacific Marine Center, Seattle WA
BECHTEL CORP. SAN FRANCISCO, CA (PHELPS)
DURLACH, O'NEAL, JENKINS & ASSOC. Columbia SC
MCDONNEL AIRCRAFT CO. Dept 501 (R.H. Fayman), St Louis MO
OCEAN DATA SYSTEMS, INC. SAN DIEGO, CA (SNODGRASS)
SHELL DEVELOPMENT CO. HOUSTON., TX (TELES)
WESTINGHOUSE ELECTRIC CORP. Annapolis MD (Oceanic Div Lib, Bryan)
WISS, JANNEY, ELSTNER, & ASSOC Northbrook, IL (J. Hanson)
WOODWARD-CLYDE CONSULTANTS PLYMOUTH MEETING PA (CROSS, III)
BRYANT ROSE Johnson Div. UOP, Glendora CA
T.W. MERMEL Washington DC